

## On Splitting and Ejection of Surface Liquid Drop Subjected to Impinging Air Jet

Kamel A. Elshorbagy<sup>1</sup>, Elhussien A. Mohammed<sup>2\*</sup>, Eslam R. Lotfy<sup>3</sup>

<sup>1</sup> Professor of Fluid Mechanics, Department of Mechanical Engineering, Alexandria University, 21544 Alexandria, Egypt

<sup>2</sup> M.Sc. Candidate in Fluid Mechanics, Department of Mechanical Engineering, Alexandria University, Egypt

<sup>3</sup> Assistant Professor of Fluid Mechanics, Department of Mechanical Engineering, Alexandria University, 21544 Alexandria, Egypt

**ABSTRACT:** The purpose of this study is to investigate the hydrodynamics of a surface liquid drop ejected downstream a plane air jet. Water was used as a base liquid and the newly created Nano-ceramic coated-glass was used as the impinging surface. The effect of the drop volume on the ejection speed and the physical regimes associated with the ejection process were investigated experimentally. The phenomenon of drop splitting was studied to find the possible reasons. An experimental method was followed to get the volume effect on the drop average velocity and splitting syndrome. Six pairs of inclination angles and offset ratios, for jet axis/impinging surface, were examined. Observations using the fast-shooting camera technique showed that the ejection and/or splitting history are largely influenced by the drop volume and the wettability between the surface and the liquid. Also, the ejection regimes depend on the drop volume, the geometrical orientation between the drop and the impinging jet and the jet velocity. The results showed that an increase of 25% in the drop volume leads to a 50% increase, on average, in the drop maximum Weber number.

**KEYWORDS:** Surface liquid drop, Air- liquid interaction, Drop ejection, Wettability, Impinging jet, Drop splitting.

Date of Submission: 04-01-2021

Date of acceptance: 19-01-2021

### I. INTRODUCTION

Transport phenomena at multi-phase interfaces represent the essence of most thermo-fluid studies. Momentum, heat, and mass transfer across gas liquid interfaces are of essential importance in such field. Impinging jets have various configurations and are widely used as a controller in numerous industrial processes. Some of the major applications include cooling of gas turbine components to withstand high temperature operation, cooling or heating of paper mill rolls, drying of tissue paper, newsprint, veneer and textile products, tempering of glass and annealing of metal or plastic sheets.

From the previous studies; the resultant of the surface tension holds not only for a sphere, but for any surface forming part of a sphere. Consider a liquid drop resting on a flat, horizontal solid surface (Fig. 1). The contact angle could be defined as the angle formed from the intersection of the solid-liquid interface and the vapor- liquid interface (this could be obtained geometrically when applying a tangent line from the contact point along the vapor-liquid interface in the drop profile). The interface where solid, liquid, and vapor co-exist was referred to as the “three-phase contact line”.

Ideally, the liquid drop shape is determined by its surface tension. In a pure liquid, each molecule in the volume is pulled equally in all directions by its neighboring molecules, resulting in a net/balance force of zero. However, the molecules at the surface exposed don't have neighboring molecules in all directions to provide a balanced net force. Instead, they are pulled inward by the neighboring molecules, as shown in Figure (1), creating an internal pressure. So, the liquid contracts its surface to keep the lowest possible surface free energy.

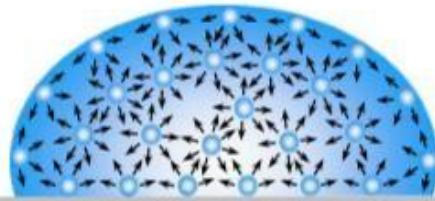


Fig. (1): Surface tension is due to unbalanced forces of liquid molecules at the surface

### Contact angle hysteresis

The phenomenon of wetting is more than just a static state. The liquid moves to expose its fresh surface and to wet the fresh surface of the solid in turn. The measurement of a single static contact angle to characterize wetting behavior is no longer adequate. If the three-phase contact line is in actual motion, the contact angle produced is called a “dynamic” contact angle. In particular, the contact angles formed by expanding and contracting the liquid are referred to as the advancing contact angle  $\theta_A$  and the receding contact angle  $\theta_R$ , respectively, as shown in figure (2). These angles fall within a range, with the advancing angles approaching a maximum value, and the receding angles approaching a minimum value. Dynamic contact angles can be measured at various rates of speed. At a low speed, it should be close or equal to a properly measured static contact angle. The difference between the advancing angle and the receding angle is called the hysteresis (H):

$$H = \theta_A - \theta_R$$

Eq. (1)

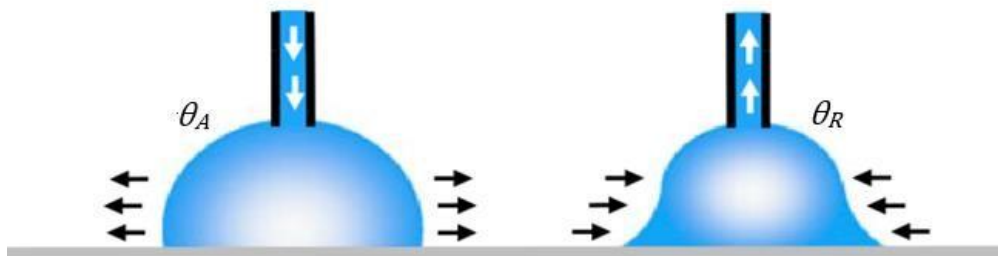


Fig. (2): An illustration of the advancing angle on the left and receding angle on the right.

The significance of contact angle hysteresis has been extensively investigated [1] and [2] and the general conclusion is that it arises from surface roughness and/or heterogeneity. For surfaces that are not homogeneous, there exist domains that present barriers to the motion of the contact line. For example, hydrophobic domains will pin the motion of the water front as it advances, causing an increase in the observed contact angle; the same domains will hold back the contracting motion of the water front when the water recedes, thus leading to a decrease in the observed contact angle. In cases that surface roughness plays the role of generating hysteresis, the actual microscopic variations of slope on the surface create barriers that pin the motion of the contact line and alter the macroscopic contact angles.

### Surface tension and splitting of liquid drops

A consequence of the free energy of a surface is that the pressure on the concave of a liquid meniscus is greater than that on the convex side. The simplest case to consider is that of a spherical surface, such as a bubble. The excessive pressure on the concave side is thus dependent on the radius of surface curvature and on the surface tension of the liquid. This theory may give a logic explanation for the separation happened in the layers subjected to a given air stream, since the air stream causes tangential and normal stresses as reported by Craik [3], Kamal [4] and Salem et al. [5]. The tangential stresses are mainly the shear stresses and normal stresses are mainly the pressure stresses, since the shear stress leads to a decrease in the layer thickness at high Reynolds number. Also, at high Reynolds number dislodging of the layer starts that causes the drop molecules to be closer to each other which gives rise to increase in the surface tension. However, as a consequence of the previous theory,  $P = \frac{2\sigma}{r}$  and since the  $r$  relation between  $P$  and  $\sigma$  is proportional to this increase tension, therefore the pressure fluctuation can give a logic explanation of the layer splitting phenomenon. Kamal [4] and Salem et al. [5] referred the drop splitting to the normal forces. Another explanation that is during increasing the jet Reynolds number, this causes the leading-edge slices to slide, passing to the trailing edge. During the sliding process, concave areas are formed in the leading-edge region, and these areas are locations of high-pressure stresses that may cause the layer splitting.

### Ripples

If gravity was taken as the sole force restoring the flatness of the gas - liquid interface  $Z = \zeta(X, Y, T)$  across that interface. The atmospheric pressure  $P_a$  is assumed continuous with the liquid pressure so that the latter's excess pressure  $P_e$  over its undisturbed value,  $P_l = P_a - \rho gZ$ , takes the boundary value  $\rho g\zeta$ ,

$$P_e = \rho l g \zeta \quad \text{Eq. (2)}$$

If this theory was modified by allowing for an additional flatness- restoring force, surface tension, which generates a discontinuity proportional to the interface curvature between the gas and liquid pressures. The resulting correction to the surface value of  $P_e$ , proportional to interface curvature, bears in comparison with the uncorrected term  $\rho g\zeta$  (proportional to interface displacement) a ratio varying as the inverse square of the wave length. Accordingly, it is important that only for those rather short waves (commonly called ripples in practice: waves of length less than around 0.1 m), however, the character of the dispersion relationship is markedly altered. Hereafter, modification to account for surface tension  $\sigma$  will be discussed in long crested wave's propagation in the  $x$ -direction.

### Vortex motion

Continuity of both tangential (no slip condition) and shear stress on the drop surface are mainly the two basic boundary conditions in the case of mass transfer (evaporation or condensation). A third boundary condition must be added, namely the continuity of mass flux across the interface. All of these conditions are responsible for the existence of vortex motion on the drop surface.

### Physical regimes associated with surface drop-plane jet interaction

Kamal [4] and Salem et al. [5] found by their experiments that the ejection process of a surface liquid drop ejected by an air stream was passing with successive phases which were highlighted by the following special features:

- 1- Semi-stagnant drop regime: which is found in the start of the air flow or at low Reynolds number, the drop in this regime is symmetric.
- 2- Small-disturbance regime: which occurs when increasing the jet velocity or accurately when the wave front of the impinging jet reached the drop surface, so a discontinuous surface waves are now presented.
- 3- Continuous-surface waves: when increasing the jet velocity more than the previous value or the wave front expanded more on the liquid surface the discontinuous waves are now turned to continuous ones, here; a weak pair of vortices are observed at the drop leading edge (L.E).
- 4- Trailing-edge ejection: increasing the jet velocity after that resulting in a fast-wave regime, these waves are propagating resulting in accelerating the secondary, weak vortices ending with the critical configuration of the drop.
- 5- Leading-edge ejection: when increasing the jet velocity, a bit more, the trailing edge (T.E) is dislodged and followed by the ejection of the L.E ending with the fully ejection.

As stated by Woodmansee and Hanratty [6]; the removal of a drop downstream an air jet is due to an imbalance between the pressure variations in the air flowing over wavelets and the stabilizing forces of gravity and surface tension, the previous section could be expressed by the stresses which are being applied in each step; firstly, at low Reynolds number, the tangential stresses –drag forces- are equal to the sum of the internal stresses due to surface tension and the friction between the liquid and solid. Increasing the jet velocity increases the drag forces, these stresses are affecting the drop surface and distorting the symmetric shape which is noticed as a discontinuity in the surface of the drop, increasing the jet velocity more pushes the air stream wave more on the surrounding of the drop resulting in continuous surface waves. The next level is achieved when the wave front affects the end of the drop i.e., the Trailing edge which is exposed to the wake effect which gives an advantage for this edge to be dislodged first. No matter, when increasing the jet velocity more, the external stresses are much larger the internal ones so; the L.E is dislodged and the drop now couldn't withstand the drag forces and fully ejected downstream the air wave.

Wierzba [7] found by examining a large number of time histories of water that in the range of Weber number from 11 to 14 there were five different basic droplet behaviors, namely: (a) flattening without breakup, (b) vibrational-type breakup, (c) bag-type breakup, (d) a behavior characteristic in the first phase for vibrational type breakup without breakup in the final phase, (e) a behavior characteristic in the first phase for vibrational type breakup and transformed into bag type breakup in the final phase.

However, the researches [1], [2] and [8] could not record the wave generation history of the water drop and recommended more mathematical and experimental investigations. In the present work; an advanced recording tool (a 24.2 mega pixel, 60 frames per second and 1/4000 shutter speed still/video camera) was used

and the recording/analyzing process was modified to capture, record and analyze the live history of the ejection process of the liquid drop. The observations coincide with the previous investigations but reveal missing sub-regimes.

The objective of this study is to investigate the physical regimes associated with the interaction of a plane air jet impinging onto a surface liquid drop as well as the phenomenon of the splitting against the previous arguments.

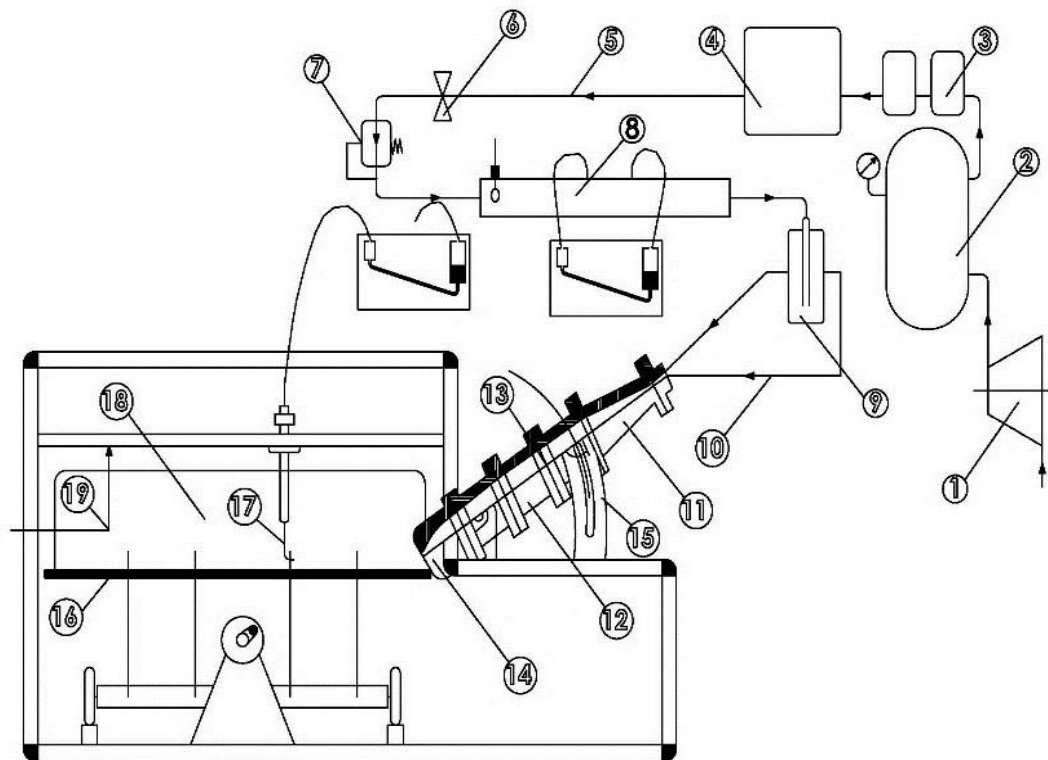
## II. EXPERIMENTAL SET-UP

The apparatus shown in figure (3) was first used by Kamal [4] and Salem et al. [5], rearranged and modified by Gawish [8] and came to the final arrangement by Elshorbagy et al. [9]

### Flow visualization techniques and measurements

The same concepts of [9] were followed to study the issues of the current investigations.

- 1- The “Nikon”, D3400 (video/still) Camera and spherical glass micro balloons (50 – 75 micrometer) were used to visualize the physical regimes of the liquid drops.
- 2- A stainless-steel Pitot-tube, calibration coefficient 0.96 with outer diameter = 1.25 mm, inner diameter = 0.9 mm (length = 25 times the outer diameter) was used to measure the jet velocity at the nozzle outlet.
- 3- The screenshots of the fixed video recordings were used to measure the drop velocity by cutting the videos using Movie Maker™.



1: Screw compressor, 2: Pressure tank, 3: Air filter, 4: Mass refrigeration air dryer, 5: Main supply pipe, 6: Main supply valve, 7: Pressure regulator, 8: Orifice meter arrangement, 9: Seven-Outlet distributor, 10: Flexible hoses, 11: Wide angle diffuser, 12: Plenum chambers, 13: Screens, 14: Elliptic contoured nozzle, 15: Adjustment mechanism of inclination angle, 16: Impingement plate, 17: Pitot-tube attached to an inclined manometer, 18: Side walls and 19: Exhaust of the spent air.

Fig. (3): Schematic diagram of the apparatus used (not to scale) [9]

### Experimental Procedure

In order to establish the different physical regimes associated with the interaction between a plane air jet and surface liquid drop, the experimental procedure of [4], [5], [8] and [9] was followed:

Where, offset ratio ( $Z^*$ ) – which is the quotient of the distance from nozzle mouth to the surface  $h$  by the nozzle outlet height  $t$  – and impinging jet inclination angle ( $\phi$ ) – which is the angle between the jet and the horizontal

surface where the drop is set.

- 1- Adjustment of ( $\phi$ ,  $Z^*$ ) to the required settings and the impinging surface horizontality
- 2- Injection of required amount of liquid using a medical syringe at the critical distance  $X_{cr}$ . Where the critical distance  $X_{cr}$  is the distance measured from the surface edge at the nozzle outlet till the position at which the drop is critical to be ejected inwards or redirected by the recirculating effects.
- 3- Starting the air flow at a fixed setting of the pressure regulator which provides the highest flow rate. The working jet Reynolds number is obtained for this setting and its value was determined as  $25.5 \times 10^3$ .
- 4- Video recording the ejection process using the plan view capturing fixed video camera.
- 5- Analyzing the data to calculate the average drop velocity.
- 6- Re-adjusting the inclination angle and measuring the corresponding offset ratio.
- 7- Analyzing the data.
- 8- Repeating for another drop volume.

The present measurements and observations were obtained for inclination angles  $\phi = 0, 15, 30$  and  $45$  degrees, and offset ratios  $Z^* = 4.5$  and  $12.63$ . These combinations of inclination angles and offset ratios ensured that the drop was always subjected to fully developed jet velocity profile. Water drop volumes were  $0.4, 0.5, 0.8$  and  $1$  milliliter. A  $\pm 0.01$ mm is the maximum estimated error of this drop height.

### III. RESULTS AND DISCUSSION

The results of the previous work [4], [5] and [9] were used to study two hydrodynamic issues related with the ejection, namely, the effect of the drop size (volume) on the ejection process and the drop-splitting phenomena, water was used as the base liquid for the test and the Nano-ceramic coated glass was used as the impinging surface, the air jet Reynolds number =  $25.5 \times 10^3$ , this results in a  $0.4553$  m/s jet velocity at the nozzle exit and the same pairs of the offset ratio  $z^*$  and the jet inclination angle  $\phi$ .

#### Critical Weber number

$$\text{Where weber number } W_b \text{ based on } U_{\max}, \quad W_b = \frac{\rho U_{\max}^2 V^{*1/3}}{\sigma} \quad \text{Eq. (3)}$$

$U_{\max}$  is the ejection velocity measured across the last regime of ejection in which the leading edge is being dislodged.

From Figures (4 a) and (4 b) it was shown that:

- 1- At the same offset ratio, higher inclination angles resulted in higher Weber number i.e., higher ejection velocities which was mentioned in [9].
- 2- For the same values of inclination angle and offset ratio, higher ejection velocities were recorded to occur in larger volumes, i.e., as the drop volume increases, the ejection speed increases. That was previously discussed in [4] and [5] but they argued that the case of  $(30^\circ, 2)$  gives the minimum wind speed needed for the start of the ejection, however, for more accurate results, more investigations were needed to give a full characterization of the phenomenon.

Figure (4 c) gives a full resultant relation for the study that:

- 1- The case  $(45^\circ, 12.63)$  resulted in the highest ejection speed and it was increasing with larger drop volumes because impingement effect is more intensive in large inclinations.
- 2- For the same drop volume, lower offset ratios,  $4.5$  cases, were confirmed to result in higher ejection velocities. This was attributed to the nature of the impinging jet in this case which subjects the closer leading part of the drop to higher tangential stresses and hence higher velocities.
- 3- The case  $(0^\circ, 12.63)$  was firmly assured to exhibit the lowest ejection speed.

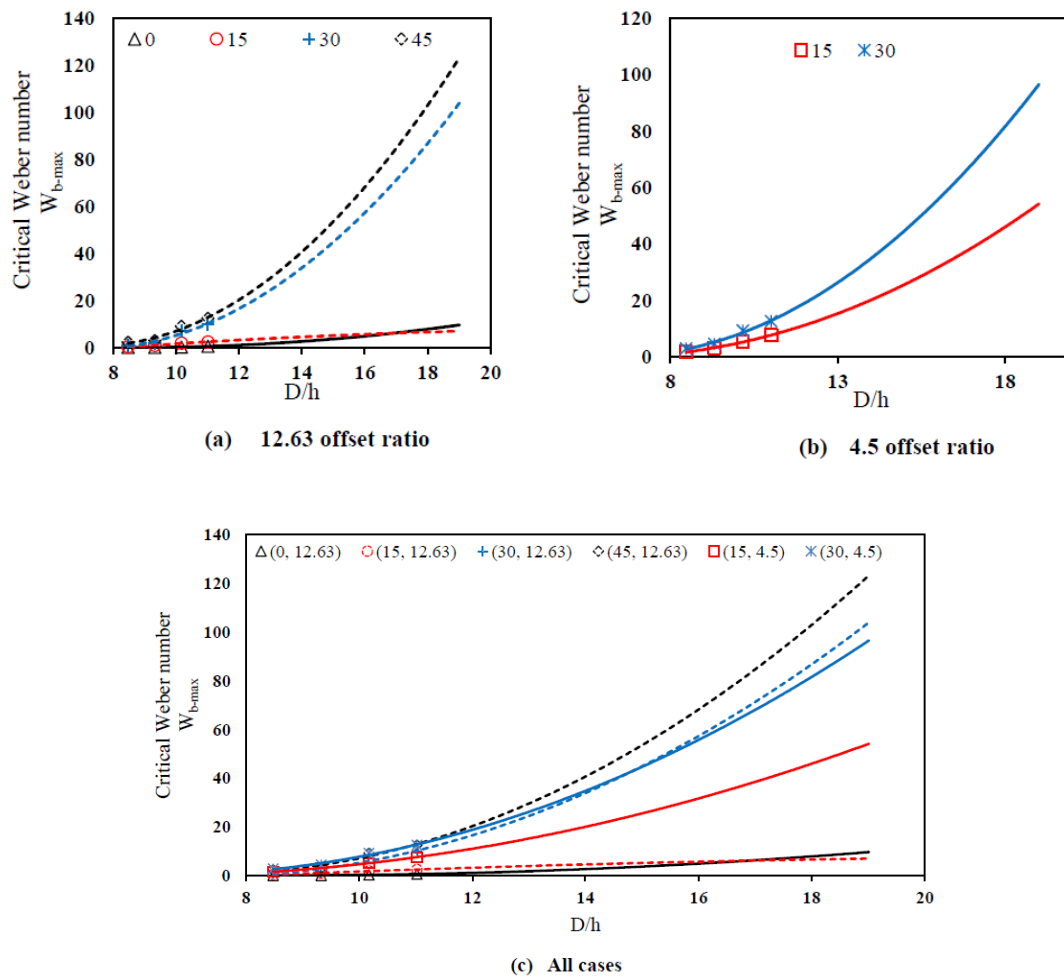
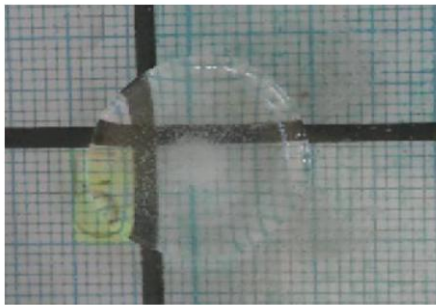


**Fig. (4): Effect of drop volume on the maximum drop velocity. The lines are 2<sup>nd</sup> degree polynomial-fitted, water drops, Nano-ceramic coated-glass surface and  $Rn = 25.5 \times 10^3$ .**

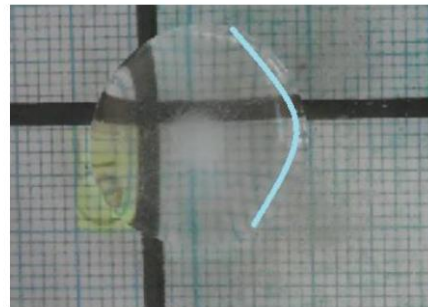
Analyzing the recorded videos for the ejection regimes; six-pairs of  $(\phi, z^*)$  and four drop volumes based on the same concept explained above; the following results and observations were found:

Figure (5) shows the consecutive screenshot of the recorded history for a 0.4ml water drop (nominally a 20cm diameter) placed on the premeasured critical distance which is 50mm for the Nano-ceramic case. The air direction is from the left to right. The micro balloons were injected with the drop and they were self-oriented at the middle due to the force equilibrium inside the drop.

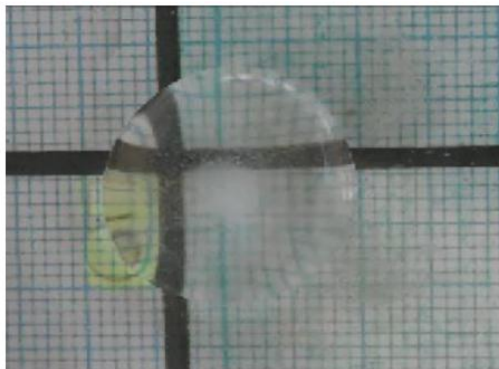
Referring that the acronyms SSW as small surface waves, CSW as continuous surface waves, V for vortex, V+CSW for vortex and continuous surface waves, D for distortion, T.E for trailing edge ejection and FULL as full ejection regime



(a) Prior the effect, stagnant drop.



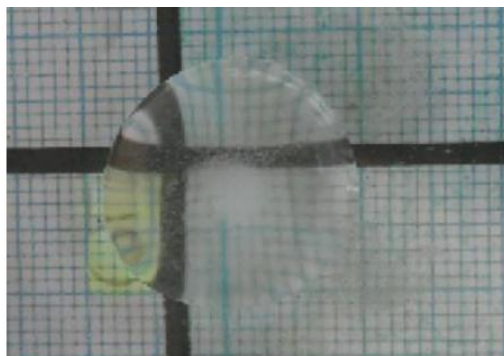
(b) Start of the impinging effect, semi-stagnant drop with crescent shape at the T.E. as predicted by [10]



(c) Small surface waves and a slight enlargement in the X-direction.



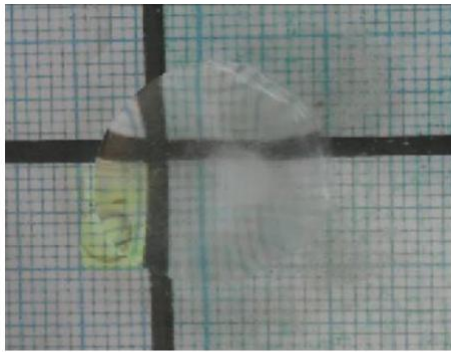
(d) Continuous surface waves: overlapping between the surface disturbances and the propagating air wave.



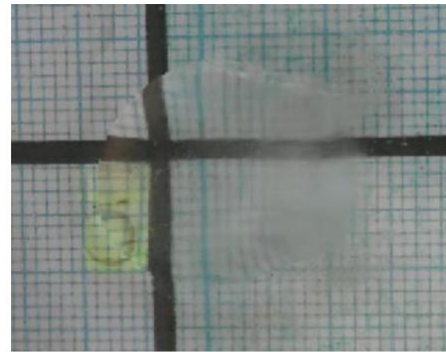
(e) The overlapping resulting in a strong vortex starting from the right-half of the drop center the nearest to the T.E., also the drop height is decreasing in the middle of the drop T.E.



(f) Propagation of the vortex towards the drop sides of the right half, continuous increase in the drop height at the T.E.



(g) Distorted drop: here the drop is being elongated in the stream direction for a 0.03sec before the starting of the ejection regimes.



(h) T.E. ejection: here the excessive stresses applied at the T.E. results in the drop dislodging under the wake effect of the air jet.



(i) Finally, the drop is fully dislodged under the drag force pushing the liquid molecules downstream the air jet.

**Fig. (5) Physical regimes of the ejection of a liquid drop downstream an air jet, the direction of air is from left to right.**

The above is the most common sequence of the ejection, the differences between cases ( $\phi, z^*$ ) are in the following parameters:

- 1- The response time in which the specific case reacted to the impinging air effect.
- 2- The time intervals between the steps by which the one could implement these configurations in a relation between the speed, case of ( $\phi, z^*$ ) and drop volume.
- 3- The reasons for drop ejection/ splitting.

However, some of these regimes, in some cases, were too short to be recorded but the main outline configuration enabled predicting these periods.

Another observation which is related only for the 0-degree inclination cases that the drop takes the shape in figure (6), these was believed to occur due to strong internal stresses towards the center of the drop though the ejection is about to starting but, in this case, the impinging effect is weak so; this shape is noticed.

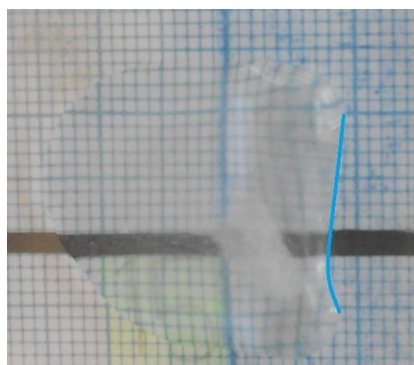
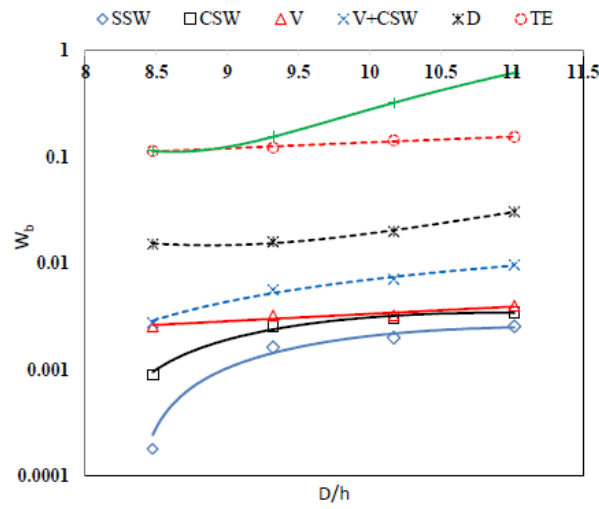
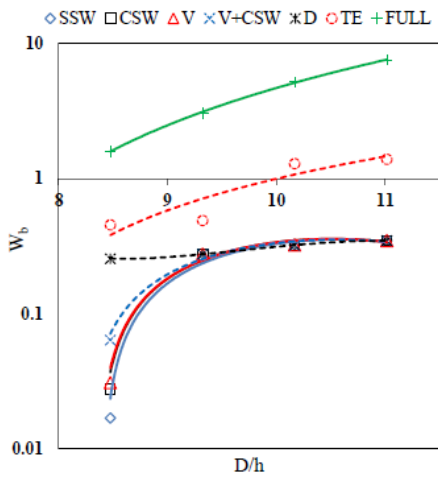


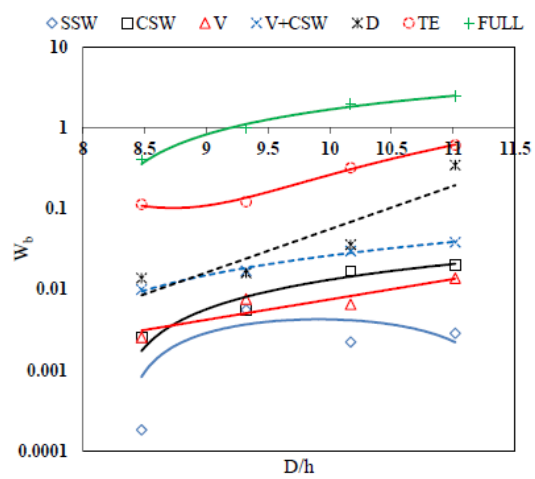
**Fig. (6) The T.E. ejection regime for a 0.5ml water drop downstream an air jet under the geometrical configuration ( $0^\circ, 12.63$ ), the air direction is from the left to right.**



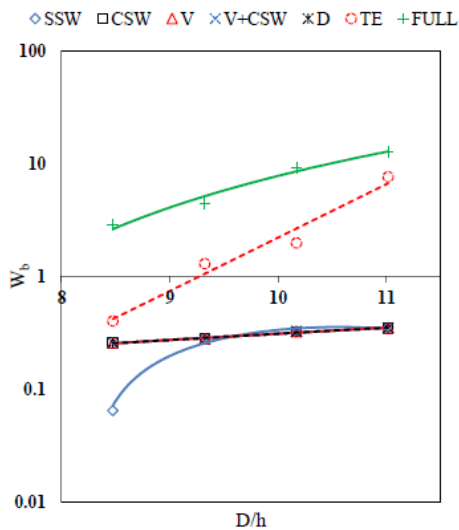
(a) Case (0°, 12.63)



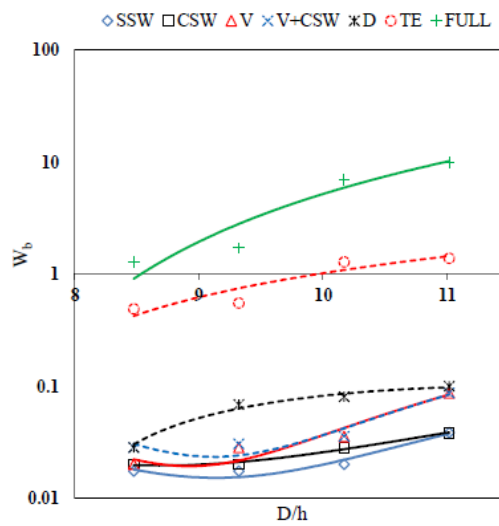
(b) Case (15°, 4.5)



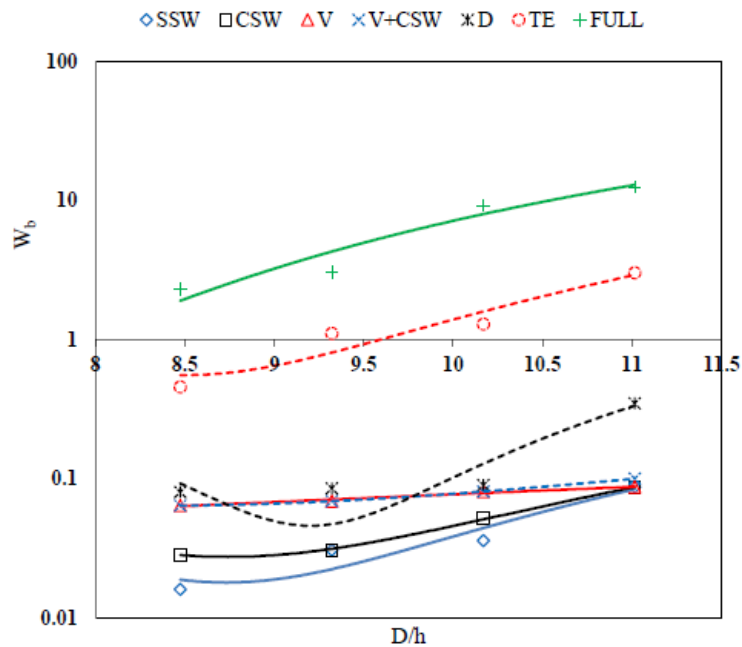
(c) Case (15°, 12.63)



(d) Case (30°, 4.5)



(e) Case (30°, 12.63)



Case (45°, 12.63)

**Fig. (7): Physical regimes associated with the ejection of a surface water drop downstream a plane air jet  $R_n=25.5 \times 10^3$  on Nano-ceramic coated-glass.**

From Figure (7); it could be observed that:

- 1- When increasing the drop volume, i.e. the ratio  $D/h$ , the speed of the drop in each stage was increased. This well agrees with the results of Kamal [4] and Salem et al. [5].
- 2- The line of the trailing edge ejection was confirmed to divide the curves of the ejection regimes into two separate zones, namely, the pre-ejection zone and the ejection zone.
- 3- The offset ratio 4.5, Figure (7 b) and (7 d), gives identical final speed in each stage because the time interval for each stage is almost the same.
- 4- In case (30°, 4.5), Figure (7 d), the pre-ejection regime lines collapse since the impinging effect is very intensive, resulting in fast-ejection regimes.
- 5- For a constant drop volume, each step of ejection displayed a higher speed than the previous stage e.g. the speed of distortion was the largest among all the pre-ejection regimes. This is because the propagation of jet waves weakens the drop resistance to dislodging.

### Phenomena of drop splitting

The splitting of a liquid drop ejected downstream an air jet occurs under specific conditions of interaction between the drop and the jet. Kamal [4] and Salem et al. [5] argued that the splitting occurs when the diameter of the liquid drop ( $D \leq 0.02$  m) and the increase in the jet speed (jet Reynolds number  $Re_d$ ) is sudden. The trailing part of drop seems to carry most of these stresses, so this may weaken the common area between the two drops and produce splitting.

Gawish [8] attributed the splitting of liquid layers to the pressure fluctuations, which may occur while increasing the jet Reynolds number, this causes the leading-edge slices to slide, passing to the trailing edge.

From the present work, the splitting was found to be due to the configuration of the ejection process itself such that for the same jet velocity and same liquid, if the any governing parameter is changed, then the resulting scenario of stagnation, splitting or ejection will be changed.

As reported by Craik [3] and Kamal [1], the tangential stresses are mainly the shear stresses, whereas the normal stresses are mainly the pressure stresses, since the shear stress leads to a decrease in the drop thickness at high Reynolds number. Under equilibrium condition, the stresses exerting on the drop are:

$$\sigma_1 + \sigma_2 = \sigma_3 + \sigma_4$$

Eq. (4)

Where  $\sigma_1$  are the shear stresses,  $\sigma_2$  are the normal stresses,  $\sigma_3$  are the internal stresses due to surface tension and  $\sigma_4$  are the stresses due to the friction between the liquid drop and the impinging solid surface at the start of the interaction process including the wettability effect.

The probabilities are:

- 1- The left-hand side of the equation is smaller than the right-hand side, then the result will be a stagnant drop, which is the case of water drop on glass, ( $0^\circ$ , 12.63) configuration.
- 2- The two sides are equal, then the drop will be critically stagnant.
- 3- The left-hand side is much larger than the right-hand side. The result will be a complete ejection.
- 4- The left-hand side is slightly larger than the right-hand side. The effect of the surface tension is strong to withstand the external stresses on the drop so, the drop takes a period of time before the ejection, during that; the external stresses exert on the trailing edge of the drop while the leading edge is exposed to the wake effect of the impinging jet, this additional stress increases the left-hand side resulting in a splitting.

From [9]; wettability affects the right-hand side that when the case is wetting i.e. the drop is spread over the surface (glass), that gives an advantage to splitting over ejection and vice versa i.e. when the case is low wettability (Nano-ceramic coated glass), the drop tends to be completely ejected.

As discussed in [4], [5] and [9], changing the geometrical configuration of the impinging jet results in variation of the tangential stresses within the drop. Therefore, for the same inclination angle, lower offset ratios are more likely to eject the drop rather than split it because the tangential stresses are larger. On the other hand, for the same offset ratio, splitting is found to take place at higher inclinations which allow the stresses on the trailing edge to be much higher than that on the leading edge. It is worth noting that the ejection velocity after splitting will be higher in this case.

The final parameter influencing splitting is the drop volume, it was found from the experiments that the larger the drop volume, drop diameter, the smaller is the chance of splitting and vice versa. This is because the internal stresses due to surface tension are weaker.

#### IV. CONCLUSION

The physical regimes associated with the ejection of a surface liquid drop by a gas jet has been examined for the effect of the drop volume and the geometrical orientation between the drop and the impinging jet. The phenomenon of the drop splitting was investigated. The studied parameters showed diverse effects on the drop ejection history. The following are the conclusions of this work,

- 1- The ejection velocity of drop is highly dependent on the volume of the drop. When drop volume increases by 25%; the drop maximum Weber number increases by 50% on average.
- 2- Every geometrical configuration of the inclination angle or the offset ratio results in a different ejection regime based on the effect of the impinging jet.
- 3- The velocity of each stage of ejection also depending on the drop volume, such that increasing the drop volume results in increasing the velocity of the vibrational motion of the drop.
- 4- The speed of ejection is propagating from the lowest values in the first stages and increasing when transporting to the ejection regimes, that the highest velocities are for the trailing-edge ejection.
- 5- The splitting of a liquid drop was explored under different conditions of wettability between the surface and liquid, the drop volume and the geometrical orientation between the drop and the impinging jet.
- 6- Liquid drop is more prone to splitting in cases of small volumes, this was introduced by [4] and [5]. 7- Intensive impinging jets tend to split the drops rather than eject it.

#### REFERENCES

- [1]. Yuan, Y., Lee, T. R.: Contact angle and wetting properties. Springer series in Surface science techniques, 51(1), 3-34 (2013).
- [2]. Kubiak, K. J., Wilson, M. C. T., Mathia, T. G., Carval, P.: Wettability versus roughness of engineering surfaces. Wear, 271(3-4), 523- 528 (2011).
- [3]. Craik, A. D.: Wind-generated waves in thin liquid films. Journal of Fluid Mechanics, 26(2), 369-392 (1966).
- [4]. Kamal, R. M. (1997) Plane air jet-surface liquid drop interaction. Dissertation, Mechanical Engineering Department, Faculty of Engineering, Alexandria University.
- [5]. Salem, E. A., Shaalan, M. R, El-Shorbagy, K.A., Radwan, M.K.: Dominant structures associated with plane jet-surface drop interaction. Proceedings of the first Pacific symposium on flow visualization and image processing, Honolulu, Hawaii. (1997).
- [6]. Woodmansee, D. E., Hanratty, T. J.: Mechanism for the removal of droplets from a liquid surface by a parallel air flow. Chemical Engineering Science, 24(2), 299-307 (1969).
- [7]. Wierzbna, A.: Deformation and breakup of liquid drops in a gas stream at nearly critical Weber numbers. Experiments in fluids, 9(1- 2), 59-64(1990).
- [8]. Gawish, A. K. M.: Plane air jet-surface water layer interaction. Dissertation, Mechanical Engineering Department, Faculty

- of Engineering, Alexandria University. (2008)
- [9]. Elshorbagy, K. A., Lotfy, E. R., Mohammed E., A.: Factors affecting surface liquid drop ejection downstream an air jet. *Journal of Scientific and Engineering Research*, 7(2), 171-184 (2020).
- [10]. Volgin, B. P., Yugai, F. S. Experimental determination of the drag coefficient of a liquid droplet in the process of deformation and breakup in a turbulent gas flow. *Journal of Applied Mechanics and Technical Physics*, 9(1), 118-120 (1968).

Kamel A. Elshorbagy, et. al. "On Splitting and Ejection of Surface Liquid Drop Subjected to Impinging Air Jet." *American Journal of Engineering Research (AJER)*, vol. 10(1), 2021, pp. 251-262.